Amphiphilic cerium(III) β-diketonate as a catalyst for reducing diesel/biodiesel soot emissions

Paulo. C. de Sousa Filho, Luciano F. Gomes, Kleber T. de Oliveira, Cláudio R. Neri, Osvaldo A. Serra *

Departamento de Química, Faculdade de Filosofia, Ciências e Letras de Ribeirão Preto, Universidade de São Paulo Av. Bandeirantes, 3900, ZIP 14040-901, Ribeirão Preto, SP, Brazil

ABSTRACT

This work reports on the synthesis, characterization and applications of the new cerium(III) β-diketonate $Ce(hdacac)_3(Hhdacac)_3 \cdot 2H_2O$ (where hdacac and Hhdacac denote, respectively, the hexadecylpentane-2,4-dionate and hexadecylpentane-2,4-dione ligands) as catalyst for the reduction of automotive emissions. Due to its amphiphilic character, this complex can be solubilized in non-polar fuels, thus generating cerium(IV) oxide particles, which efficiently catalyze the oxidation of diesel/biodiesel soot.

The synthesized complex was characterized by microanalysis (C, H), thermal analysis, and infrared spectroscopy. Scanning electron microscopy, X-ray diffractometry, and specific surface area measurements attested that the complex can act as a soluble precursor of homogeneous CeO_2 spherical nanoparticles. The efficiency of this compound as catalyst for the reduction of soot emission was evaluated through static studies (comprising carbon black oxidation), which confirmed that increasing concentrations of the complex result in lower carbon black oxidation temperatures and lower activation Gibbs free energies. Dynamic studies, which embraced the combustion of diesel/biodiesel blends containing different amounts of the solubilized complex in a stationary motor, allowed a comparative evaluation of the soot emission through diffuse reflectance spectroscopy. These analyses provided very emphatic evidences of the efficiency of this new cerium complex for the control of soot emission in diesel/biodiesel motors.

© 2009 Published by Elsevier B.V.

1. Introduction

Diesel is, by far, the most commonly employed fuel for energy generation in high potency motors. This is due to its efficiency compared with other conventional fuels and to the durability of the diesel-operated motors [1]. However, its limited availability (non-renewable fuel) and the environmental problems associated with its use have led to the development/introduction of biodiesel as a potential substitute for diesel [2–7].

On the other hand, one of the main problems related to the use of diesel or diesel/biodiesel blends in compression motors is the high degree of generation of particulate material, composed basically by soot derived from incomplete combustion. So, current research involving the building of more efficient motors, the development of better fuels, and the treatment of exhaust effluents is widely impelled by environmental concerns and increasingly stricter legislations. In this sense, cerium-based catalysts have received evergrowing attention from researchers in this field [1,8–11]. The commonest of these catalysts is based on the action of

cerium(IV) oxide (ceria), which is a remarkable material due to its redox properties arising from a non stoichiometric behaviour [1]. For example, ceria is an important component of the commercial TWC's (three-way catalysts, consisting of a ceramic substrate doped with Pt/CeO_2 sites), which has a short lifetime but high catalytic efficiency in diesel motors [12]. In compression motors, where there is high oscillation in the air/fuel ratio, this compound favors oxidation of the effluents resulting from incomplete combustion, acting as an oxygen regulator. Eqs. (1)–(3) show its activity in a simplified way:

$$2CeO_2 + C \rightarrow Ce_2O_3 + CO \tag{1}$$

$$2CeO_2 + CO \rightarrow Ce_2O_3 + CO_2 \tag{2}$$

$$Ce_2O_3 + O_2 \rightarrow 2CeO_2 \tag{3}$$

In addition, the presence of CeO_2 can promote the conversion of CO into hydrocarbons and water, besides converting nitrogen oxides into N_2, showing very promising results [1,8–14]. In most of these cases, the contact between CeO_2 and the effluents is obtained by adequate supporting of this oxide on porous ceramic substrates (through which the combustion products flow) or by addition of the catalyst to the fuel in the form of an additive (an organometallic

compound) [1,9,14,15]. The second alternative allows for a more efficient association between the involved species [1,8,11]. The introduction of the additive in the motor can be performed by injection after the ignition chamber (which leads to the aggregation of the CeO_2 with the soot particles), or by dispersing the precursors in the fuel before the combustion takes place. The latter seems to be more advantageous, because this process favors a homogeneous catalyst nucleation. Besides that, CeO_2 particles can also act as nuclei for soot deposition. Moreover, these additives may be associated with catalytic filters, contributing to the regeneration and to the prolongation of the lifetime of the latter [1,8,11].

The major difficulty encountered in the utilization of these additives is, however, optimization of the solubility and stability of the precursors. Aiming at these applications, this work deals with the development of a new cerium-based fuel additive, capable of reducing the emission of soot generated in diesel/biodiesel combustion. Taking into account the widely studied chelating properties of β-diketones [16], we have synthesized and characterized a cerium(III) complex of the 3-hexadecylpentane-2,4-dione (Hhdacac) ligand, whose properties allow solubilization of lanthanide(III) ions in non-polar solvents [17]. Thus, this amphiphilic β-diketonate can introduce cerium(III) ions in diesel/biodiesel blends and, therefore, act as a homogeneous precursor of a heterogeneous catalyst (CeO_2). Its catalytic activity has been determined by static (carbon black oxidation) and dynamic studies (combustion of additived diesel/biodiesel blends), in which a simple method was employed for the comparative evaluation of soot emission.

2. Experimental

2.1. Synthesis and characterization of Ce(hdacac)$_3$(Hhdacac)$_3$·2H$_2$O

The synthesis and the characterization of the hexadecylpentane-2,4-dione ligand and its corresponding Eu^{3+} complexes has been described in the literature [17]. The synthesis of Ce(hdacac)$_3$(Hhdacac)$_3$·2H$_2$O was performed by applying the same methodology as the one used for the Eu^{3+} complexes [17], but $CeCl_3$ solutions (prepared from the dissolution of CeO_2 99.995%, Aldrich, in concentrated hydrochloric acid with additions of hydrogen peroxide, pH ∼3) were employed instead of $EuCl_3$ solutions. In summary, the complex was precipitated from a water:ethanol 1:1 solution containing $CeCl_3$ and the sodium salt of Hhdacac (Ce^{3+}:hdacac = 1:1), pH ∼6.5 (35 °C, 12 h, under stirring).

The composition of the complex was determined by microanalysis in a Carlo Erba Instrument EA 1110 analyzer. The infrared spectra (FT-IR) were recorded in a PerkinElmer 502 spectrophotometer from 4000 to 400 cm^{-1} (resolution of 2 cm^{-1}), in KBr pellets. The cerium percentage and the thermal behaviour of the complex were investigated in a Thermal Analyst 2100-TA Instruments STD 2690-Simultaneous DTA-TGA, operating under synthetic air or N_2 atmosphere, with a heating rate of 10 °C min^{-1}.

In order to evaluate some morphological aspects of the CeO_2 generated by this precursor, a solution of the Ce^{3+} complex (4 mg L^{-1} of Ce^{3+}) in a diesel/biodiesel blend (98:2, v/v) was heated at 400 °C for 1 h, which initiated decomposition of the organic fraction. The decomposition was completed through calcination at 900 °C in air for 2 h. The obtained powder (cerium(IV) oxide) was characterized by X-ray diffractometry (XRD) in a Siemens D5005 diffractometer (using Cu-Kα radiation, 1.541 Å), and its morphological analysis was carried out in a Zeiss EVO 50 scanning electron microscope (SEM). The specific surface area (SSA) of the prepared cerium(IV) oxide sample was calculated through the Brunauer–Emmet–Teller method (BET) [18,19], by using high purity nitrogen

as adsorbate and liquid nitrogen as refrigerating bath in a Quantachrome NOVA 1200 instrument.

2.2. Static studies (carbon black oxidation)

The potential of the synthesized complex as catalyst was firstly evaluated by studies on the combustion of mixtures containing Ce(hdacac)$_3$(Hhdacac)$_3$·2H$_2$O and carbon black (CB) (Printex® U, Degussa) by thermal analysis.

Appropriate amounts of the solid complex and CB were mixed in an agate ball mill for 45 min. These mixtures were then submitted to thermal analyses under synthetic air atmosphere with a heating rate of 10 °C min^{-1}.

In the present studies, only small amounts of catalyst were added to the soot sample (i.e., the mixtures presented large excess of CB). The quantities of the solid complex added for these tests were calculated considering the literature [20] and the Brazilian Petroleum, Natural Gas and Biofuel National Agency (ANP) data, which state that diesel combustion results in the generation of 0.2–0.5% of the initial mass as soot. In these experiments, the combustion of 1 L of diesel or of a diesel/biodiesel blend (with densities around 0.85 g mL^{-1}) was considered to result in the formation of 2500 mg soot (about 0.3%). The solid mixtures were prepared in order to simulate the concentrations of 2, 4, 6, and 10 mg L^{-1} of Ce^{3+} in the fuel. So, the concentrations of Ce^{3+} in carbon black calculated for this analysis were 800, 1600, 2400, and 4000 ppm.

2.3. Dynamic studies (combustion of diesel/biodiesel blends)

The catalytic action of the cerium(III) β-diketonate was evaluated through tests comprising the combustion of fuels containing different amounts of solubilized Ce(hdacac)$_3$(Hhdacac)$_3$·2H$_2$O. Various diesel/biodiesel blends were prepared (in volumes: 100:0 (B0), 98:2 (B2), 95:5 (B5), 85:15 (B15) and 70:30 (B30)), to which different amounts of the complex were added so as to achieve Ce^{3+} concentrations of 2, 4, and 6 mg L^{-1}. The mixtures were prepared under stirring and mild heating (∼45 °C) for 1 h. The diesel samples were acquired from the Petrobrás Petroleum Terminal at Ribeirão Preto, SP, Brazil, and the biodiesel samples (obtained from methanolic transesterification of soy oil [21]) were supplied by the Fuel and Materials Laboratory of the University of Brasília, Brazil.

The combustions were performed in a stationary motor (Branco BD-5.0H) coupled to a generator group (Branco B4T-2500), operating at maximum acceleration and at a consumption regime of 1500 W. The effluents produced in the combustion process were directed to a quantitative paper filter (80 g m^{-2}) placed at the end of the motor exhaust tube. This arrangement is shown in Fig. 1.

In the combustion experiments, the motor was kept running in a pre-heating process for 30 min. The filters were then exposed to the soot emitted at the end of the exhaust tube for 15 min; the experiments were performed as triplicates. The impregnation of soot in the exposed filters was evaluated by diffuse reflectance spectroscopy [22,23]. The spectra were acquired (from 350 to 900 nm) in a NanoCalc 2000 UV–vis/NIR reflectometer (detection angle = 90°, 4.4 cm of distance from the sample to the sensor and an integration time = 18 ms).

3. Results and discussion

3.1. Characterization of Ce(hdacac)$_3$(Hhdacac)$_3$·2H$_2$O

The percentage of Ce^{3+} in the obtained complex, determined by complexometric titration (with standard edta solution and xylenolorange as indicator), is 6.10/6.60 (found/expected). The
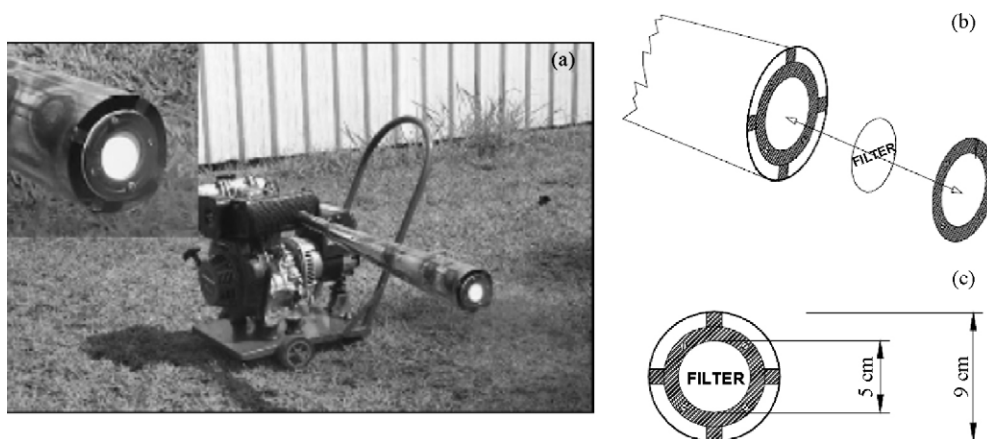
Fig. 1. (a) Photography of the apparatus (stationary motor and generator) developed for the diesel/biodiesel additive blend combustions (inset: end of the exhaust tube); (b and c) schematization (with the main measures) of the filter support at the end of the exhaust tube.

thermogravimetric analysis led to a Ce^{3+} percentage of 7.04 in the complex. Data from microanalysis attests for a carbon percentage of 72.4 (expected: 71.3%) and for a hydrogen percentage of 12.1 (expected: 11.5%). The analysis show little discrepancies from the theoretical values for the proposed formula (Ce(hdacac)$_3$(Hhdacac)$_3$·2H$_2$O). This is a consequence of the unsatisfactory drying of the complex prior to the analyses, since it is a waxy and thermally unstable solid, and of the fact that the complex is a kind of non-stoichiometric compound, once there is a relatively variable number of neutral ligand (Hhdacac). This is possibly due to the amphiphilic character of the ligand which, upon complex isolation, results in the establishment of hydrophobic interactions between the aliphatic chains. This results in metal/ligand ratios greater than 1:3 (which are the commonest for rare earth β-diketonates [16]), which can be considered as ∼1:6 (i.e., three ionic ligands – 3-hexadecylpentane-2,4-dionate – balancing the metal charge, and three neutral ligands – 3-hexadecylpentane-2,4-dione – maintained by hydrophobic interactions).

Another identical aspect observed for the Eu^{3+} [17] and Ce^{3+} complexes is the infrared absorption profile. Fig. 2 displays the FT-IR spectra of the cerium(III) β-diketonate and the free Hhdacac ligand. The Hhdacac FT-IR spectrum displays the two characteristic carbonyl bands of 1,3-diketones (symmetric and anti-symmetric stretchings) at 1724 and 1706 cm^{-1}. The other remarkable bands, which can be ascribed to the enolic form of this β-diketone, are the small and broad band at ∼3500 cm^{-1} of hydrogen bonded OH
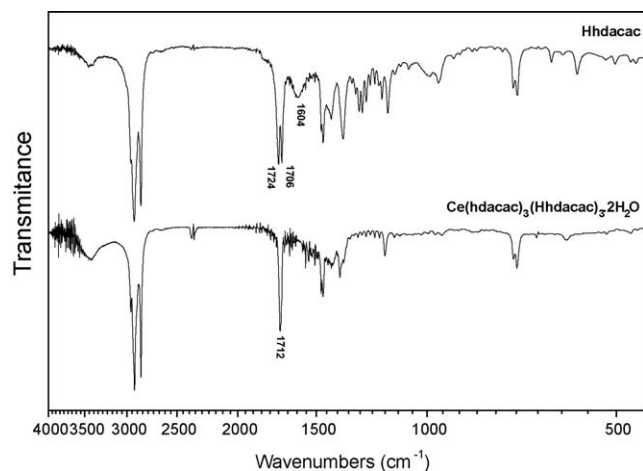
groups and the little intense carbonyl conjugated C=C band at 1604 cm^{-1}. In the Ce^{3+} complex, besides an alteration of the "fingerprint region" profile and the appearance of residual water OH bands, there is a superposition of all carbonyl stretchings, which occurs as a single band at 1712 cm^{-1}. This also provides evidence that the ligands are coordinated to the metal centre through the oxygen atoms. In addition, the absence of the band at 1604 cm^{-1} indicates that the Hhdacac groups occur in the keto form in the complex.

3.1.1. Thermal behaviour

Fig. 3 displays the thermal behaviour (TGA, DTG and DTA) of the cerium(III) β-diketonate under oxidizing (synthetic air) and inert (N$_2$) atmospheres. In both cases, an endothermic peak in the DTA curve without appreciable mass variation is observed (at ∼53 °C), which can be ascribed to solid melting. In oxidizing conditions, the TGA curve is similar to that of the previously synthesized Eu^{3+} complex [17], in which three major weight loss steps (all of exothermic nature) at 150–255 °C, 255–340 °C, and 350–460 °C are observed. The total weight loss is 91.40%, which is coherent with the following percentages of Ce^{3+} in the complex: 7.04/6.60 (found/expected for Ce(hdacac)$_3$(Hhdacac)$_3$·2H$_2$O). The first decomposition step can be associated with the partial ligand decomposition and water loss; the two last steps can be ascribed to the total decomposition of the remaining ligands and possible oxycarbonates formed during the analysis, besides Ce^{3+}/Ce^{4+} oxidation. This analysis shows that, in oxidizing conditions, the β-diketonate can act as a precursor of cerium(IV) oxide at reasonably low temperatures (below 500 °C).

Under non-oxidizing conditions, there are two weight loss steps, both with exothermic nature (presenting, however, smaller values of temperature difference compared with the analysis under synthetic air). These steps correspond to volatilization and partial ligand decomposition, leading to a cerium(III) carbonate residue (11.16%/10.83%, found/expected for Ce$_2$(CO$_3$)$_3$).

3.1.2. Cerium(IV) oxide particles

In order to evaluate the morphological properties of the cerium(IV) oxide generated by fuel additivation with Ce(hdacac)$_3$(Hhdacac)$_3$·2H$_2$O, a combustion was simulated in laboratory conditions. Fig. 4 shows the SEM micrographs of the solid obtained (after calcination) from the combustion of the B2 blend containing 4 mg L^{-1} of Ce^{3+} in the β-diketonate form.

The images show that the solid is composed by micrometric aggregates of very thin layers (<3 μm). The amplifications reveal that the sheets are built up by homogeneous quasi-spherical nanoparticles, with diameters between 25 and 100 nm. The
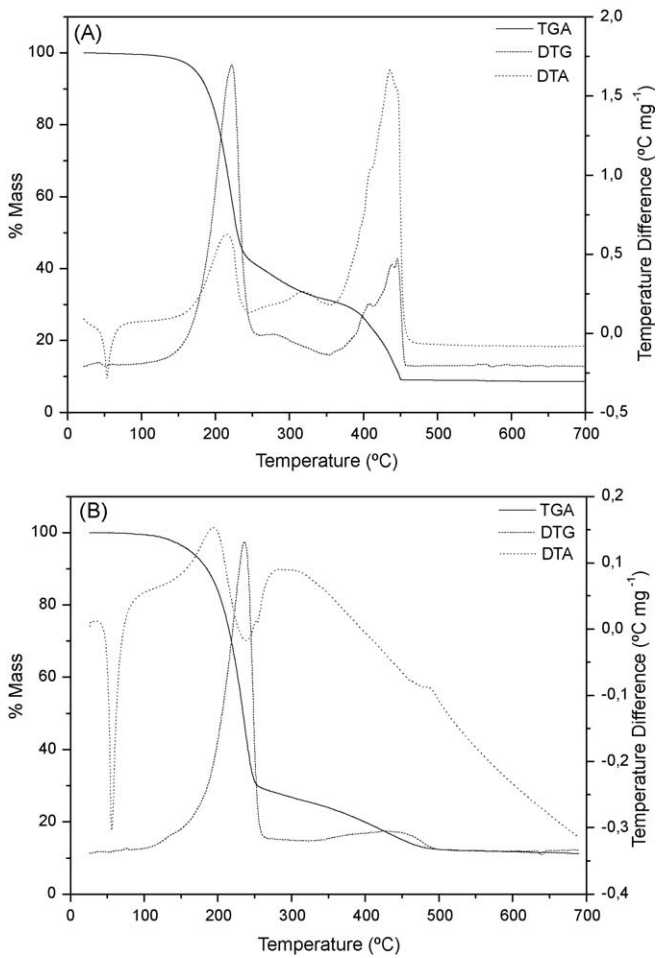

Fig. 2. Infrared spectra (KBr pellets) of the Hhdacac ligand and the complex Ce(hdacac)$_3$(Hhdacac)$_3$·2H$_2$O.

Fig. 3. Thermal analysis (TGA, DTG and DTA) under (A) oxidizing atmosphere (synthetic air), and (B) inert atmosphere (N_2). (DTA: Exo up).

occurrence of nanostructures with a low size range indicates that there is a fast and homogeneous nucleation step in the combustion process. This is an important factor for this kind of fuel additive once the contact between the catalyst and the soot is increased.

Fig. 5a shows the XRD pattern of the solid obtained after the calcinations. The diffraction lines confirm that the obtained solid is cerium(IV) oxide, once they are coherent with the characteristic face centered cubic Fluorite structure (whose spatial group is $Fm3m$) of this compound. The mean crystallite size of this solid was estimated from the XRD analysis through the Scherrer method (considering the (1 1 1) and (2 2 0) reflections), and the obtained
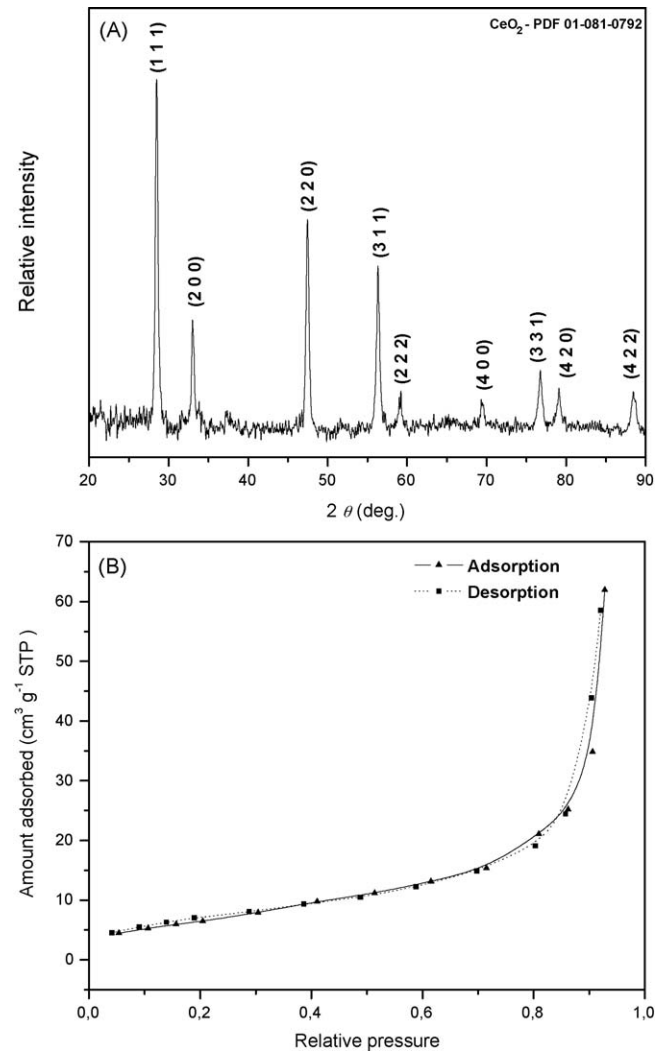

Fig. 5. (A) Powder X-ray diffractogram and (B) BET adsorption/desorption isotherms of the obtained CeO_2.

values are around 23 nm, which also attests that the material has nanosized structure.

The BET adsorption/desorption isotherms (Fig. 5b) have a sigmoidal profile, which agrees with the occurrence of a non-porous material or a micro-porous solid [19]. The curves do not present any significant hysteresis (which is expected only for micro-porous materials); this confirms the low porosity of the obtained CeO_2. However, the structure shows some kind of pores as a result of the aggregation of the spherical particles (thus
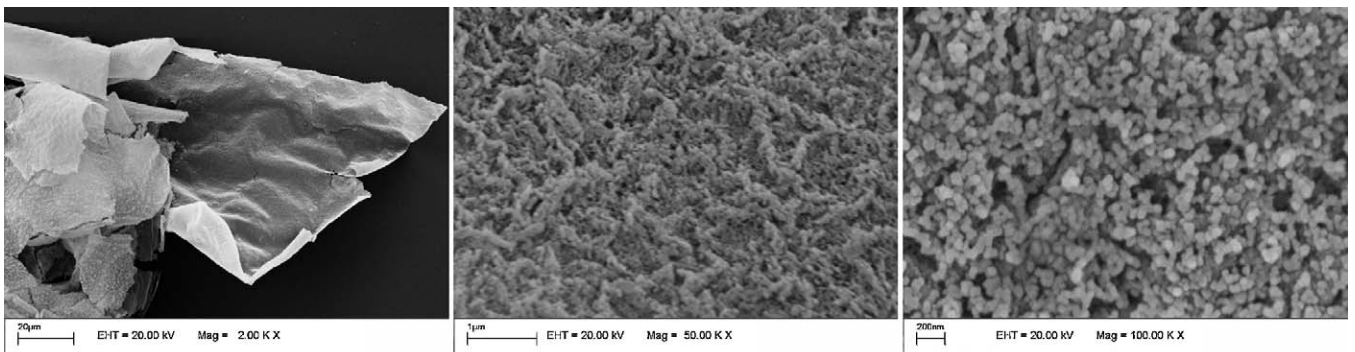

Fig. 4. Scanning electron micrographs of CeO_2 obtained by combustion/calcination of B2 additived with 4 mg L^{-1} of Ce^{3+} as $Ce(hdacac)_3(Hhdacac)_3\cdot2H_2O$.

generating free spaces in the solid structure). Applying the software apparatus (NOVA Gas Sorption Analyzer 5.01), these pores are estimated to have about 150 Å (mesopores). The mean SSA (obtained treating the BET isotherms data with the mentioned software) for this solid is 25 $m^2 g^{-1}$. This value of superficial area, which does not seem to be very high for solid catalysts, does not correspond to the real available area of the CeO_2 nanoparticles when they are generated as a dispersion in the fuel once, in the latter case, the aggregation degree is much lower. Since the measurement of SSA was carried out after elimination of organic residues and calcination at 900 °C, the particles may have undergone strong coalescence processes, which diminished the total area of the solid.

3.2. Influence of the complex on carbon black oxidation

As explained in the experimental section, the catalytic potential of the synthesized complex was evaluated by thermal analyses of mixtures of carbon black (CB) and $Ce(hdacac)_3(Hhdacac)_3 \cdot 2H_2O$ (in ratios that simulate concentrations of 2, 4, 6, and 10 mg L^{-1} of Ce^{3+} in the fuels). Fig. 6 shows the thermal decompostion curves of the prepared mixtures and the respective derivatives.

Fig. 6 shows that the sample corresponding to pure CB remains stable up to ~450 °C, and its decomposition occurs with maximum rate at ~632 °C (DTG peak), in a single step. At about 653 °C, the pure CB sample is completely decomposed. The addition of increasing amounts of the complex results in the progressive reduction of the DTG peak temperature, not to mention that the residues of the decompositions are stabilized at lower temperatures. One can thus affirm that the complex is capable of reducing the temperature of CB oxidation.

The DTG curves also show that more than one decomposition step takes place with increasing additions of the complex. Moreover, the intimate mixture between CB and the catalyst leads to thermal stabilization of the complex once, in contrast with the pure complex, no decomposition steps are seen below 450 °C. Thus, for higher Ce^{3+} concentrations, the occurrence of more than one DTG peak can be ascribed to the degradation of the organic fraction of the complex, oxidation of Ce^{3+} to Ce^{4+}, and CB oxidation.

For a better evaluation of the properties of the synthesized β-diketonate, the kinetic parameters involved in CB oxidation in the presence of the compound were estimated from the thermal analyses by applying the Coats–Redfern method (Eq. (4)) [24–26]:

$$\log\left(\frac{g(\alpha)}{T^2}\right) = \log\left[\frac{AR}{\Phi E_a}\left(1 - \frac{2RT}{E_a}\right)\right] - \frac{E_a}{2.303RT} \qquad (4)$$

where T is the temperature, A is the pre-exponential factor, R is the gas constant, Φ is the heating rate, and E_a is the activation energy. The algebraic expression of the $g(\alpha)$ function depends on the mechanism of the solid state reaction that takes place during the thermal decomposition. The activation entropies, enthalpies, and Gibbs free energies were also calculated [25] for each mixture with the determined values of A and E_a. The mechanisms of thermal
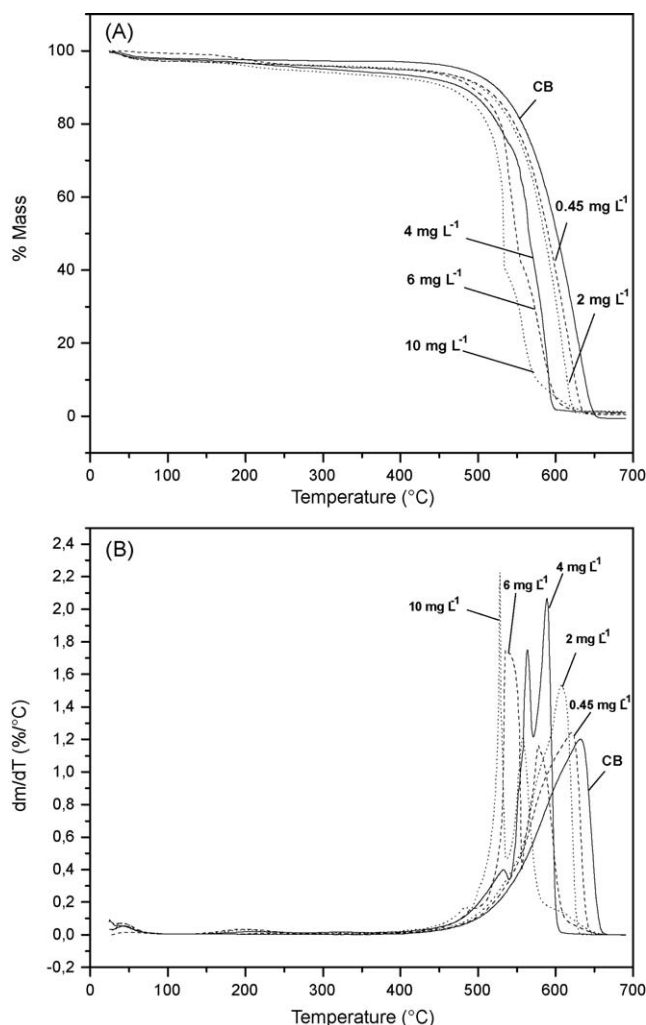

Fig. 6. (A) TGA and (B) DTG curves of the different mixtures containing CB and the cerium(III) β-diketonate.

decomposition of the CB/complex mixtures can be assigned by using many forms of $g(\alpha)$ for fitting the decomposition profiles and by evaluating the obtained correlation coefficients. The function $g(\alpha)$ for which the correlation is the highest corresponds to the most probable thermal decomposition mechanism and shall be used for calculation of the kinetic parameters. Table 1 shows the correlation coefficients obtained for the thermal degradations by considering nine forms of $g(\alpha)$ [25,26]

The results show that the decomposition of pure CB is better correlated with the $g_4(\alpha) = (1 - 2/3\alpha) - (1 - \alpha)^{2/3}$ function, whose corresponding solid state reaction mechanism is a three-dimensional diffusion (Ginstling–Brounshtein equation) [26]. However,

Table 1
Correlation factors for the thermal decomposition of CB/complex samples obtained by using nine forms of $g(\alpha)$ functions [25,26].

| $g(\alpha)$	CB	0.45 mg L^{-1}	2 mg L^{-1}	4 mg L^{-1}	6 mg L^{-1}	10 mg L^{-1}
$g_1(\alpha) = \alpha^2$	0.98966	*0.99960*	*0.99957*	*0.99795*	*0.99566*	*0.99582*
$g_2(\alpha) = \alpha(1-\alpha)\ln(1-\alpha)$	0.99121	0.98532	0.99248	0.99216	0.99075	0.99311
$g_3(\alpha) = [1 - (1-\alpha)^{1/3}]^2$	0.99274	0.98342	0.98357	0.98606	0.98153	0.98547
$g_4(\alpha) = (1 - 2/3\alpha) - (1-\alpha)^{2/3}$	*0.99993*	0.99800	0.98746	0.99184	0.98102	0.98001
$g_5(\alpha) = -\ln(1-\alpha)$	0.99204	0.99414	0.98698	0.98470	0.98958	0.98815
$g_6(\alpha) = [-\ln(1-\alpha)]^{1/2}$	0.98832	0.97954	0.98249	0.97438	0.97396	0.98024
$g_7(\alpha) = [-\ln(1-\alpha)]^{1/3}$	0.98591	0.97650	0.97367	0.97138	0.97203	0.97634
$g_8(\alpha) = 1 - (1-\alpha)^{1/2}$	0.99226	0.98216	0.96989	0.98640	0.98301	0.97688
$g_9(\alpha) = 1 - (1-\alpha)^{1/3}$	0.98702	0.97839	0.96525	0.98006	0.97934	0.96753
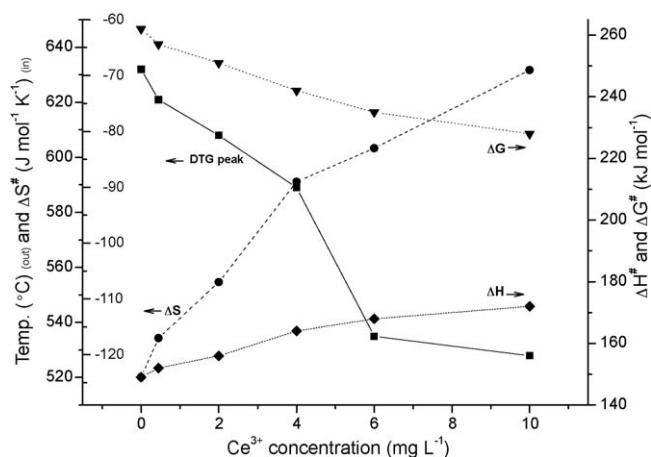
Fig. 7. Influence of the cerium(III) complex content on the CB oxidation temperature and on the entropies, enthalpies and Gibbs free energies of activation.

addition of increasing amounts of the complex alters the decomposition mechanism, which is attested by the better fitting for the $g_1(\alpha) = \alpha^2$ function (corresponding to a one-dimensional diffusion reaction mechanism [26]). This observation is coherent with the appearance of more than one DTG peak related to the thermal degradation of the prepared mixtures.

Table 2 displays the observed DTG peaks and the calculated kinetic parameters of the CB/complex mixtures. As observed, additions of Ce(hdacac)$_3$(Hhdacac)$_3$·2H$_2$O result in expressive reductions of the CB oxidation temperature. Table 2 data are organized in a graph (Fig. 7), which clearly shows the effects of the β-diketonate on the kinetic parameters of CB decomposition.

Although a decrease in CB oxidation temperatures is observed, the calculations show an unexpected increase in the activation energies with the addition of the synthesized compound. This occurs because the cerium(III) complex itself is not catalytically active; the catalyst is, in fact, the CeO$_2$ generated in its combustion. So, with the addition of the complex, higher activation energies are required once a larger amount of complex may be decomposed/ oxidized. However, the larger amounts of CeO$_2$ produced in the presence of high complex concentrations result in lower CB oxidation temperatures. Moreover, the data in Table 2 and Fig. 7 also show that, although there is an increase in the activation energies, the processes becomes less endergonic with increasing additions of Ce(hdacac)$_3$(Hhdacac)$_3$·2H$_2$O (which is evidenced by a reduction in the activation Gibbs free energies). Therefore, in the overall process, less energy is required for CB oxidation in the presence of the β-diketonate, which can be considered an active compound in soot oxidation.

3.3. Combusiton of diesel/biodiesel blends

The general principle of the Bosch method [27] was employed for the qualitative evaluation of soot emission. If one holds a paper filter at the end of the exhaust tube, the amount of particulate material retained at the filter surface is proportional to its concentration in the effluents from the combustion of a fuel sample; so, an adequate measurement of the amount of soot deposited on the filter provides a direct indication of the degree of soot emission. This measurement can be accomplished, for example, through gravimetric methods, which are not very suitable due to experimental inconveniences. Thus, we have applied a simple spectroscopic technique (based on diffuse reflectance measurements) in order to compare the soot emission of different samples.

The soot emitted from diesel combustion is a carbonaceous material with intense absorption in the visible range of the electromagnetic spectrum. In a filter exposed to the effluents of combustion, the absorbance is as high as the soot concentration. Hence, higher amounts of soot lead to higher absorbance and, consequently, to lower percentage of diffuse reflectance. In this case, the generated particulate material was estimated through comparisons between measures of diffuse reflectance (DR) of the
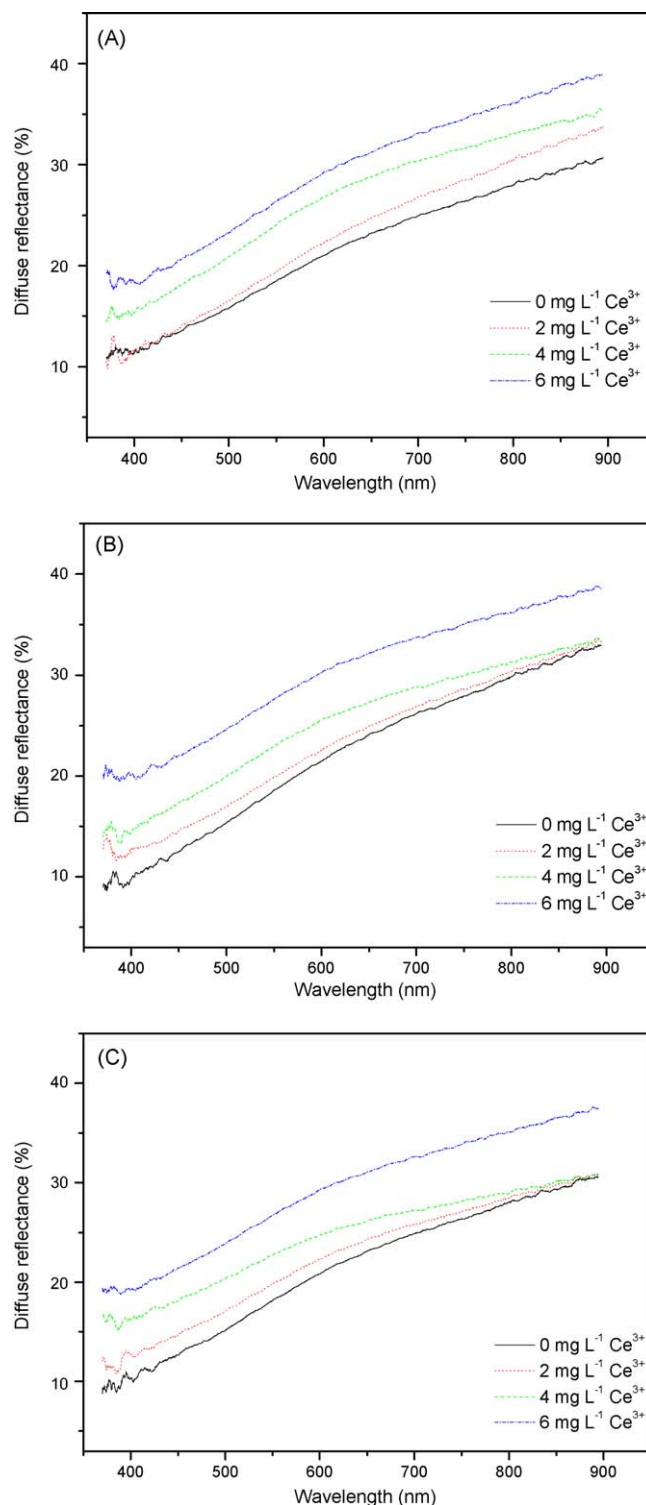

Fig. 8. Diffuse reflectance spectra of the filters exposed to the combustion of (A) B0, (B) B2, and (C) B5 with different amounts of the cerium complex.

Table 2
DTG peaks, activation energies, pre-exponential factors, and entropies, enthalpies and Gibbs free energies of activation calculated for the thermal decomposition of CB/complex samples.

CB/Ce^{3+}	DTG peak (°C)	E_a (kJ mol^{-1})	A (s^{-1})	$\Delta S^{\ddagger}$ (J mol^{-1} K^{-1})	$\Delta H^{\ddagger}$ (kJ mol^{-1})	$\Delta G^{\ddagger}$ (kJ mol^{-1})
100:0 (0 mg L^{-1})	632	142	6.08×10^6	−124	149	262
100:0.02 (0.45 mg L^{-1})	621	145	1.45×10^7	−117	152	257
100:0.08 (2 mg L^{-1})	608	149	4.47×10^7	−107	156	251
100:0.16 (4 mg L^{-1})	589	157	3.45×10^8	−89	164	242
100:0.24 (6 mg L^{-1})	535	161	7.53×10^8	−83	168	235
100:0.40 (10 mg L^{-1})	528	166	4.21×10^9	−69	172	228

impregnated samples and the blank filters (DR = 100%). The measurements were carried out for B0, B2, B5, B15, and B30 without additives and with additivation of 2, 4 or 6 mg L^{-1} of Ce^{3+}. Fig. 8 shows the DR spectra obtained for the combustions of B0, B2, and B5 with different amounts of the complex.

The DR spectra of the filters impregnated with soot display the same spectral profile, but the increase in the percentage of diffuse reflectance with the addition of the complex evidences the reduction in soot emission. The DR spectra relative to B10, B15, and B30 displays essentially the same profile and same tendency (increase in DR percentage with higher Ce^{3+} concentrations), which attests for the catalytic activity of the synthesized β-diketonate.

In all DR spectra, the 300–350 nm and 700–900 nm wavelength ranges present a low signal/noise ratio and thus low confidence. So,

we have selected to consider fixed intermediate wavelength values for the comparisons between the obtained spectra (550 and 650 nm). Fig. 9 shows the DR percentages at these wavelengths for each of the prepared samples.

Fig. 9 summarizes the information obtained from the DR spectra of the filters exposed to the motor effluents. In this experiment, the increase in the amount of biodiesel in the fuel blend leads to a higher emission of particulate material (evidenced by lower DR percentages). Particularly, the combustion of the blends B15 and B30 results in larger emissions of particulate material, except for the higher Ce^{3+} concentrations. Addition of 2 mg L^{-1} Ce^{3+} as complex has little influence on soot emission in relation to the combustion of the pure fuels. Nevertheless, addition of a few milligrams of cerium(III) in the form of Ce(hdacac)$_3$(Hhdacac)$_3$·2H$_2$O (mainly 6 mg L^{-1}) to the fuels results in expressive reductions in soot emissions (evidenced by increases of up to 15% in DR measurements). This confirms the catalytic action of the β-diketonate on the redox processes involved in the combustions.

4. Conclusion

The amphiphilic properties of the 3-hexadecylpentane-2,4-dione ligand allow the for the production of metal complexes with appreciable solubility in non-polar solvents. This characteristic enables the development of metal fuel additives, which are capable of acting as homogeneous precursor for the treatment of combustion effluents. The cerium(III) complex obtained here – Ce(hdacac)$_3$(Hhdacac)$_3$·2H$_2$O – was characterized with respect to its ability to function as CeO$_2$ precursor and as a reducer of soot emission in diesel/biodiesel combustions. The analyses have shown that this β-diketonate leads to the formation of homogeneously dispersed CeO$_2$ nanoparticles. Its catalytic activity was confirmed by static studies, in which the oxidation temperatures of CB samples were notably reduced upon addition of small amounts of the complex. The dynamic studies (which comprised the combustion of diesel/biodiesel blends with different amounts of the complex and the comparative evaluation of the particulate material emission with a spectroscopic method) have attested for the catalytic activity of Ce(hdacac)$_3$(Hhdacac)$_3$·2H$_2$O, once the degree of soot emission was diminished in the presence of this compound. Thus, this new cerium(III) coordination compound is a very promising component of fuel additives designed for the reduction of soot emission by diesel/biodiesel motors.
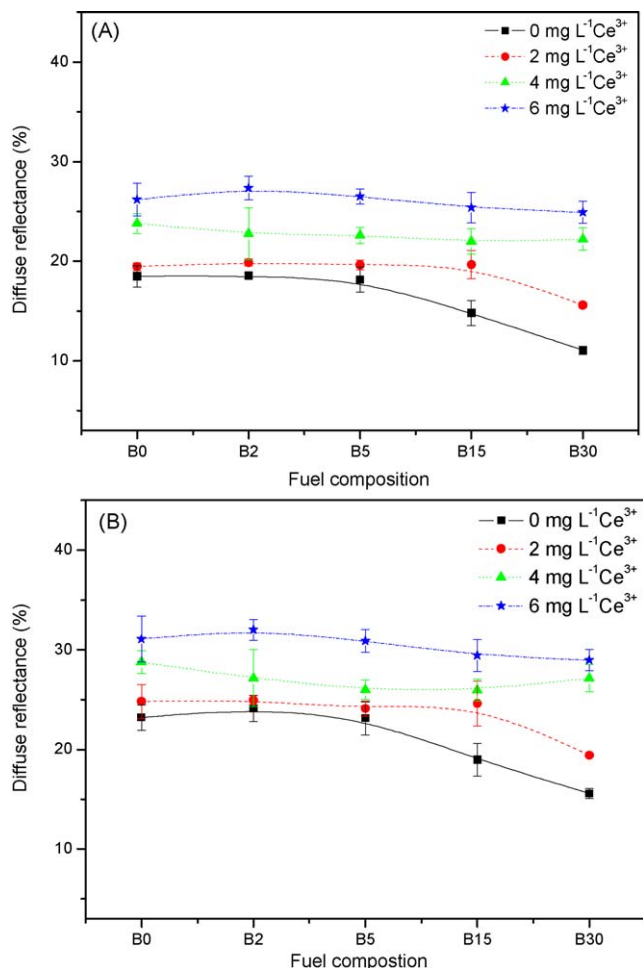
Fig. 9. Diffuse reflectance percentages in (A) λ = 550 nm, (B) λ = 650 nm for B0, B2, B5, B15, and B30 with different Ce^{3+} concentrations. (Filter: DR = 100%).

References

[1] A. Trovarelli (Ed.), Catalysis by Ceria and Related Materials, Imperial College Press, London, 2002, , Chapters 2, 7, 10 and 12.
[2] E.G. Shay, Biomass Bioenerg. 4 (4) (1993) 227–242.
[3] M.S. Graboski, R.L. McCormick, Prog. Energy Combust. Sci. 24 (1998) 125–164.
[4] H. Fukuda, A. Kondo, H. Noda, J. Biosci. Bioenerg. 92 (5) (2001) 405–416.
[5] D.Y.Z. Chang, J.H. Van Gergen, I. Lee, L.A. Johnson, E.G. Hammond, S.J. Marley, J. Am. Oil Chem. Soc. 73 (11) (1996) 1549–1555.
[6] R. Altin, S. Çetinkaya, H.S. Yücesu, Energy Convers. Manage. 42 (2001) 529–538.
[7] J. Hill, E. Nelson, D. Tilman, S. Polasky, D. Tiffany, Proc. Nat. Acad. Sci. 103 (30) (2006) 11206–11210.
[8] A. Trovarelli, C. Leitenburg, M. Boaro, G. Dolcetti, Catal. Today 50 (1999) 353–367.
[9] J. Lahaye, S. Boehm, P.H. Chambrion, P. Ehrburger, Combust. Flame 104 (1996) 199–207.
[10] R.J. Farrauto, R.M. Heck, Catal. Today 51 (1999) 351–360.
[11] J.P.A. Neeft, M. Makkee, J.A. Moulijn, Fuel Proc. Technol. 47 (1996) 1–69.
[12] S.E. Golunski, H.A. Hatcher, R.R. Rajaram, T.T. Truex, Appl. Catal. B-Environ. 5 (1995) 367–376.
[13] S. Hilaire, X. Wang, T. Luo, R.J. Gorte, J. Wagner, Appl. Catal. A-Gen. 258 (2004) 271–276.
[14] E.E. Miró, F. Ravelli, M.A. Ulla, L.M. Cornaglia, C.A. Querini, Catal. Today 53 (1999) 631–638.
[15] S.J. Jelles, R.R. Krul, M. Makkee, J.A. Moulijn, Catal. Today 53 (1999) 623–630.
[16] K. Binnemans, in: K.A. Gschneidner, Jr., J.-C.G. Bünzli, V.K. Pecharsky (Eds.), Handbook on the Physics and Chemistry of the Rare Earths, Elsevier, Amsterdam, 2005, , Chapter 225.
[17] L.F. Gomes, K.T. de Oliveira, C.R. Neri, P.C. de Sousa Filho, M.J. Dal Bianco, A.P. Ramos, M.E.D. Zaniquelli, O.A. Serra, J. Lumin. 128 (2008) 1339–1347.
[18] S. Brunauer, P. Emmett, E. Teller, J. Am. Chem. Soc. 60 (1938) 309–319.
[19] K. Sing, Colloid Surf. A 187 (2001) 3–9.
[20] J. Xi, B. Zhong, Chem. Eng. Technol. 29 (2006) 665–673.
[21] J.S. Oliveira, R. Montalvão, L. Daher, P.A.Z. Suarez, J.C. Rubim, Talanta 60 (2006) 1278–1284.
[22] F.A.A. Matias, W.A. de Oliveira, E. Moschim, Sens. Actuators B-Chem. 41 (1997) 159–162.
[23] F.A.A. Matias, M.M.D.C. Vila, M. Tubino, Sens. Actuators B-Chem. 88 (2003) 60–66.
[24] A.W. Coats, J.P. Redfern, Nature 201 (1964) 68–69.
[25] E.A. Faria, A.G.S. Prado, React. Funct. Polym. 67 (2007) 655–661.
[26] A.O. Moura, A.G.S. Prado, J. Col. Int. Sci. 330 (2009) 392–398.
[27] A. Faiz, C.S. Weaver, M.P. Walsh, Air Pollution from motor vehicles – Standards and technologies for controlling emissions, The World Bank, Washington, D.C, 1996, Chapter 4.